Yale
NsG-407

INTERPLANETARY SCINTILLATION IN JOVIAN DECAMETRIC RADIATION

JAMES N. DOUGLAS and HARLAN J. SMITH

The University of Texas

Received

ABSTRACT

Spaced-receiver observations over four oppositions establish the origin of the one-second component of time-structure in Jupiter's decametric emission as diffraction by inhomogeneities in the solar wind moving radially outward from the sun. Arguments from simple diffraction theory suggest inhomogeneity correlation scale sizes ranging from a few hundred to a few thousand kilometers, and set an upper limit on the intrinsic angular size of Jupiter's decametric source at about 5".

I. INTRODUCTION

Rapid fluctuations have been a puzzling feature of the decametric radiation from Jupiter since its discovery by Burke and Franklin in 1955. Because many of the fluctuations are one to two orders of magnitude faster than the radio-source scintillations arising from diffraction by terrestrial ionospheric electron clouds, the fast fluctuations were originally attributed to intrinsic time variations of the source on Jupiter. In turn, this stimulated a variety of theoretical models of sources capable of producing such rapid time variations (plasma oscillations, lightning discharges, etc.). However, Gardner and Shain (1958), with two receivers separated by 25 km on an E-W line, produced simultaneous records showing poor correlation of fluctuations having a time scale of seconds or larger, reopening the possibility of some ionospheric process though presumably a different one from that responsible for the well-known slower radio-source scintillations. Several groups have studied these phenomena, especially at Florida and Chile (see e.g. Carr et al. 1964) and at Colorado (Warwick 1963).

In 1958 the newly formed radio astronomy group at Yale, hoping to use Jupiter fluctuations as a tool for measuring dispersion in the interplanetary medium (Phillip 1957), established a continuing spaced-receiver experiment to determine the origin of the fluctuations; some preliminary reports of findings have appeared (Smith and Douglas 1958a, 1962; Smith, Lasker and Douglas 1960; Douglas and Smith 1961, 1963a,b,c; Douglas 1960, 1963, 1964). The present paper details our observations of one class of fluctuations in the Jupiter radiation — the L-pulses — and offers evidence

strongly supporting the hypothesis (Smith and Douglas 1962; Douglas 1963, 1964) that most if not all of the L-pulses arise from diffraction by inhomogeneities in the solar wind.

II. SUMMARY OF TIME STRUCTURE

On reception at the earth, Jovian decametric radiation is characterized by a hierarchical time structure (see e.g. discussion and references cited in Douglas 1964). A five-level classification is suggested by single-frequency records of flux versus time, illustrated in Figures 1-4.

Hourly average flux values during a one-month time interval are plotted in Figure 1, showing narrow spikes of one to three hours duration (noise storms) appearing in groups lasting several days to one week (activity periods). The sharply discontinuous apparent character of the noise storm arises primarily from a sampling effect caused by observing a periodically stimulated directive rotating emitter with a directive rotating receiver; the presence of pronounced activity periods arises in part from the same cause, and may also reflect some intrinsic time variation of the source.

In a noise storm (e.g. Figure 2) there is a strong tendency for apparent activity to be concentrated into periods of several minutes duration (burst groups); much of this appearance is produced by terrestrial ionospheric scintillation, but dynamic spectra (Warwick 1963) show that concentration into frequency drifting burst groups on this time scale must

be due to time variation or frequency-dependent directivity of the source on Jupiter.

Each burst group in turn normally consists of a series of pulses unresolved at typical slow recording speeds. The high-speed photographic record of Figure 3 resolves such a burst group, showing the spikes of Figure 2 to be composed of one or more peaks (L-pulses), each having a duration on the order of one second. Although frequently the L-pulses are the fastest structure observed in a storm, sometimes more rapid structures (S-pulses) with durations ranging from less than 0.01 to 0.1 second appear to be superimposed on the L-pulses (Figure 4). The terminology used here, mainly introduced by Gallet (1961), is summarized in Table 1.

Table 1.

The above simple hierarchy is not always obvious in the observations; Figures 1 - 4 were chosen for clarity. Among the more frequent deviations from this classification scheme are noise storms in which burst groups are difficult to distinguish (although the L- and S-pulse fine structure may remain present), and relatively weak noise storms which appear to contain no fluctuations whatever.

III. OBSERVATIONS OF L-PULSES

a) Equipment

The observations to be discussed in this paper are records of flux versus time, obtained at 22.2 Mc/s and adjacent frequencies with receivers at five locations. The principal receiver and the recording equipment for all receivers were located at the Bethany Observing Station of the Yale Observatory. Other receivers were located on the campus of Wesleyan University, Middletown, Connecticut; at the Pomfret School, Pomfret, Connecticut; at Hendrie Hall on the campus of Yale University, New Haven, Connecticut; and at the Kalbfleisch Field Station of the American Museum of Natural History, Huntington, Long Island. Table 2 gives the coordinates of each station together with the azimuth and distance of each relative to the Bethany station. Azimuths are expressed in terms of the horizon system of 72° 18!6 west longitude, 41°40!8 north latitude, which was chosen so that Bethany, Pomfret and Huntington all lie in a plane parallel to the horizon plane. In this system, Middletown has altitude 7.7 minutes of arc and Hendrie Hall -37.1 minutes of arc.

Table 2.

For various reasons, one or more receivers have been omitted from the full system each year; Table 3 summarizes the frequencies and stations in operation on a year-by-year basis.

Table 3.

All 22.20 Mc/s receivers were of similar design, utilizing crystal-controlled local oscillators and 6 kc/s bandwidth mechanical filters to insure frequency stability. The other receivers at Bethany utilized stable variable-frequency local oscillators to establish the operating frequencies; actual operating frequency was periodically checked with a frequency standard.

All receivers used identical horizontally polarized 8-element Yagi antennas. The Bethany antenna was tracked on Jupiter; the others were adjusted to suitable directions every several months. The strength of Jupiter storms is such that records of adequate quality were obtained over a four hour time span around the time when Jupiter crossed the beam of the fixed antennas. Automatic diode-noise-generators in parallel with the antennas produced, for each receiver, hourly calibration marks used primarily to verify proper receiver and antenna operation.

Audio noise from each remote receiver was carried to the Bethany Observing Station over voice-type telephone circuits having, for these purposes negligible, propagation delays. Noise from all receivers was rectified, integrated for approximately 10 milliseconds, and amplified; the resulting DC voltages deflected the galvanometers in a Honeywell Visicorder high-speed photographic recorder. One-second time lines and WWV ticks were recorded simultaneously with the fluctuating DC voltages from the receiver-rectifier systems at chart speeds normally of 0.2 inch/second (Figure 3), but with 1 inch/second (Figure 4) and 5 inch/second speeds occasionally used.

The continued synoptic monitoring program (Douglas and Smith, 1963 a,b) utilized interferometers which permitted unambiguous identification of Jupiter emission, so that the pulses seen on the spaced receivers and analyzed in this paper are definitely known to be associated with Jupiter emission.

b) Time Correlation of L-Pulses at Different Frequencies

A given L-pulse normally has a band-width of the order of several megacycles (see also Warwick 1963; Smith et al. 1963). Careful measurements of times of L-pulse peaks at two frequencies have been made on single-station high speed records from three storms in 1960 (0.8 Mc/s spacing) and three storms in 1964 (0.4 Mc/s spacing). No departures from simultaneity within the measuring accuracy of 0.05 sec were noted during the 20 minute average duration of these storms.

A tendency for burst groups to drift up or down in frequency has been noted by several observers (see particularly Warwick 1961, 1963; also Smith, Lasker and Douglas 1960; Douglas, 1960; Carr et al. 1961). A single-station high speed multi-frequency record was obtained of a drifting burst group on 29 March 1960; Figure 5 was derived from this record. Each L-pulse is resolved and is seen to occur simultaneously over a range of frequencies; the frequency drift of the burst group is manifested through changing weightings of the individual L-pulses.

Thus, we find that simultaneous arrival of L-pulses over a megacycle range is typical, whether or not they make up a frequency drifting burst group, indicating a different mode of origin for L-pulses and burst groups.

c) Spatial Correlation

L-pulse correlation between the receivers spaced at separations up to 100 km was frequently found to be excellent (Figures 3 and 4); of 79 storms rich in L-pulses which were examined, each exhibited at least some degree of long-baseline correlation. However, typically the best correlation between records of the spaced receivers requires small but distinct time shifts, e.g., in Figure 3, the Pomfret record is virtually identical to the Bethany record, but the amplitude structure occurs 0.30 seconds later.

The most extensive available correlations between the Bethany and Pomfret stations are at 22.2 Mc/s. These records, covering four apparitions of Jupiter, have been analyzed in two ways. First, the time delays for some 25 to 100 pairs of L-pulses for each storm observed at Bethany and Pomfret were measured and used to construct a delay histogram, permitting estimation of the most frequently occuring delay. Second, deflections on 14 of the 79 records were measured every $0^{s}.25$, and analyzed numerically with cross-correlation techniques. Time delays obtained by the two methods are in excellent agreement. Table 4 summarizes the results of both types of measurements.

Table 4.

The general prevalence of fraction-of-a-second lags over many tens of kilometers suggests an origin of the L-pulses in an irregular pattern of brightness and shadow which is drifting at several hundred kilometers per second more or less along the Bethany-Pomfret line. The characteristic

scale size of the bright patches in this pattern would be the duration of L-pulses times the velocity, or a few hundred kilometers.

This interpretation is supported by four-station observations obtained in 1961. Bethany, Middletown, and Pomfret are approximately in a line; and Hendrie is at right angles to this line. The delay histograms for 30 April 1961 are shown in Figure 6. Note that the lags over the 99 km Pomfret-Bethany distance were substantially larger than those for the 31 km Middletown-Bethany distance, also that the lags over the perpendicular Hendrie-Bethany line were systematically zero on this date. Although the Hendrie-Bethany distance is insufficient to prove that the drift velocity was accurately along the Bethany-Middletown-Pomfret line, it does rule out the otherwise possible hypothesis that the observed lags might have been produced by a pattern of slow-moving thin strips oriented at a small angle to the Bethany-Pomfret line.

The drifting isophotal pattern implied by these observations requires a certain degree of time-stability to produce such well-correlated but time-delayed records as Figure 3; specifically, the characteristic time for change in the isophotal pattern producing Figure 3 must be substantially greater than the observed delays ($\sim 0^{s}.3$). The data as a whole require that the stability time of the average pattern be in excess of one second; however, a number of series of L-pulses show rather poor envelope correlation which may be a result of more rapid time variation of the pattern.

IV. ORIGIN OF THE DRIFTING ISOPHOTAL PATTERN

In the previous sections we have attributed the origin of the L-pulses to the passage of an irregular isophotal pattern of typically 500 km scale-size past the receiver at velocities of several hundred km/sec. The pattern has similar contours and velocity over at least a 5% frequency range, and normally remains stable in a drifting coordinate system for at least one second. Such a drifting pattern may arise in three general ways:

1. Fine-structured directivity in the source
2. Random distribution of absorbing clouds along the line of sight, moving with an appropriate velocity component perpendicular to the line of sight, or
3. A similar distribution of irregularities producing phase shifts only.

In the following sections, it will be shown that only mechanism (3) may be reconciled with the observations and other relevant astronomical information.

1. Fine-Structure Source Directivity

Synoptic and dynamic spectrum observations of Jupiter (Warwick 1963) suggest that the emission is beamed with radiation confined to a cone of width on the order of 20°. Existence of very much smaller beams within this primary cone could produce the required isophotal pattern in space. A receiver on the earth would appear to be translated through this pattern at a rate determined by the combined effect of orbital motions and rotations of earth and Jupiter. To produce the observed scale size of the L-pulse isophotal pattern on earth, important

changes in emitted flux must occur in angles on the order of 500 km/4 a.u. or ~ 0.1. In turn such a directivity would require source coherence size greater than 10^6 wavelengths (15,000 km). While not ruled out by direct observations as yet, so large a coherent source lacks physical plausibility.

A second and more significant difficulty with this hypothesis arises from considerations of drift velocity. If the source rotated with the planet, Jupiter's rotation period of about 10 hours would correspond to a pattern drift velocity at the orbit of the earth of approximately 10^5 km/sec at opposition, three orders of magnitude greater than the observed velocities. Thus, any hypothetical large coherent source may not partake of Jupiter's rotation. While the well-known correlation of occurrence probability of radiation with Jovian longitude (e.g. Douglas 1964) does not absolutely require the source to rotate with the planet or its magnetosphere, nevertheless this remains by far the most obvious interpretation. In the absence of supporting evidence for a large non-rotating source, such a model must be considered unlikely.

2. Random Distribution of Absorbing Clouds

One of the most familiar instances of a drifting isophotal pattern occurs on a partly cloudy day when the sun's light is obscured by an irregular pattern of drifting cumulus. If analogous drifting absorbing clouds are to cause the L-pulses, they may not be in co-rotating portions of Jupiter's atmosphere or magnetosphere, because of the velocity problem considered above. If anywhere in the vicinity of the earth, such clouds must have a scale size of 500 km; if in the

ionosphere, they would subtend an angle of 60°, and would produce L-pulses on cosmic noise and all discrete radio sources. But observations of Cyg A and Cas A at the Bethany Observing Station show no evidence of L-pulses whatever. In the case of Cyg A, this requires that such clouds be sufficiently distant that their angular size be less than that of Cyg A. Using one minute of arc as Cygnus' angular scale, we require a distance of much more than $2(10)^6$ km or 300 earth radii.

By excluding hypothetical absorbing clouds from the near vicinity of earth and Jupiter, we have made their presence in any location extremely unlikely. To produce attenuation by absorption or critical reflection, electron densities some five orders of magnitude higher than those associated with the interplanetary medium would be required.

3. Random distribution of phase-changing irregularities.

A random distribution of electron density inhomogeneities will impose phase fluctuations on incoming wavefronts, thereby producing a diffraction pattern. The usual ionospheric scintillation is a result of this process; the isophotal patterns produced have scales on the order of kilometers and drift velocities on the order of tenths of a kilometer per second. Ionospheric origin of L-pulses may be ruled out by the arguments of section 2 - specifically the observed scale size of the L-pulse isophotal pattern and the failure of Cygnus A to exhibit L-pulses; the effective diffracting screen must be more than 300 earth radii away. Similarly, the previously used velocity argument excludes co-rotating portions of Jupiter's atmosphere from consideration. Thus, diffraction by inhomogenieties

in the interplanetary medium is indicated.

The ratio of root-mean-square flux to mean flux in a Jupiter storm is usually of the order of unity, i.e. the fluctuations carry a signicant fraction of the average flux. Under such conditions, the root-mean-square phase fluctuation Φ_o produced in the wavefront must be on the order of or greater than one radian (Ratcliffe 1956; Mercier 1962; Briggs and Parkin 1963). For inhomogeneities with root-mean-square correlation scale size r_o kilometers and with root-mean-square electron density deviation ΔN per cubic centimeter,

$$\Phi_o \approx \frac{.0006}{f_{mc}} r_o \Delta N \sqrt{n} \qquad (1)$$

where f_{mc} is the observing frequency in megacycles per second and n is the number of inhomogeneities in the line of sight. At 22.2 mc/s, then, we require

$$r_o \Delta N \sqrt{n} \geq 37000 \text{ km/cm}^3 \qquad (2)$$

This inequality may be readily satisfied along a 4 astronomical unit line of sight in the interplanetary medium; we shall therefore consider in detail the hypothesis of origin of L-pulses in an interplanetary diffraction process.

V. DIFFRACTION IN THE INTERPLANETARY MEDIUM

The intermittent presence of outward moving solar plasma in the interplanetary medium has been established for years, notably by studies of the correlation of solar activity and geomagnetic phenomena. Evidence of a general streaming of particles out from the sun has accumulated

beginning with Biermann's 1951 study of acceleration in Type I comet tails and culminating in direct measurement of solar wind velocity and density from spacecraft. The almost invariable appearance of L-pulses in Jupiter emission requires the continuous presence of a diffracting medium in the line of propagation; we will accordingly concentrate our attention on the continuing solar wind component of interplanetary plasma.

Observations made with the positive-ion spectrometer on Mariner II have established basic properties of the solar wind between 0.7 and 1.0 a.u. (Snyder, Neugebauer and Rao 1963; Neugebauer and Snyder 1965). Radial-velocity components were generally between 360 and 700 km/sec, and number densities between 0.3 and 10 proton/cm^3. Important systematic variations in velocity were noted, corresponding to passage of the spacecraft through streams of high velocity plasma. While velocities of these streams were closely correlated with geomagnetic disturbances, no systematic change in radial velocity with distance from the sun was observed over the range 0.7 to 1 a.u. The solar wind pressure at 0.7 a.u. was approximately twice its value at a.u, as one would expect in view of the constant velocity. The kinetic energy of the solar wind was much greater than magnetic energy as measured on board the same spacecraft; essentially radial velocities are therefore suggested.

Electron-density inhomogeneities are required for the diffraction process; each Mariner II measurement represents a spatial average over many thousands of kilometers, and small-scale inhomogeneities would not have been seen. Evidence for the existence of irregularities is provided by observations of occultations of radio stars by the outer solar corona (Hewish 1955, 1958; Vitkevitch 1960,1961; Slee 1961; Erickson 1964). The

phenomenon observed is an increase in apparent angular size of the source due to scattering; the irregularities are considered to be in a diffracting slab in the solar corona. The irregular phase of the emergent wave may be considered to give rise to plane waves propagating into a cone of half-width α_o radians about the original direction of propagation (see e.g. Ratcliffe 1956). If the spatial auto-correlation function of electron density is

$$\exp\ (-r^2/r_o^2), \text{ then}$$

$$\alpha_o = \frac{\lambda}{\pi r_o}\ , \quad \Phi_o < 1 \tag{3}$$

$$\alpha_o = \frac{\lambda \Phi_o}{\pi r_o}\ , \quad \Phi_o > 1 \tag{4}$$

A point source will appear to have an angular size α_o, which may be measured with suitable equipment, yielding r_o if $\Phi_o < 1$ and r_o/Φ_o if $\Phi_o > 1$. Observations of α_o at two different wavelengths determine the applicable range of Φ_o : if $\Phi < 1$, α_o = constant λ; if $\Phi > 1$, α_o = constant λ^2. Observations show that within about 100 radii of the sun, α_o = constant λ^2, and therefore $\Phi_o > 1$. This fact was used by Hewish and Wyndham (1963) to show that $r_o > 50$ km at 90 solar radii. The same authors, arguing that the angular size of the irregularities must be smaller than α_o, found that $r_o <$ 5000 km at 60 solar radii. Thus, at 1/2 a.u. inhomogeniety scale sizes of a few hundred to a few thousand kilometers are consistent with observations.

Erickson (1964) has obtained an empirical relation for α_o between 5 and 60 solar radii based on occultation observations of Taurus A at 26 Mc/s:

$$\alpha_o = \frac{50\ \lambda^2}{R_o^2} \qquad \text{minutes of arc,} \tag{5}$$

where λ is the observing wavelength in meters, and R_o is the distance of closest approach of the line of sight to the sun in solar radii. Assuming that this represents in an approximate way conditions R_o radii from the sun, we may use (1), (4) and (5) to write for our observing wavelength

$$\Delta N \sqrt{n} = \frac{470}{R_{au}^2} \tag{6}$$

where R_{au} is expressed in astronomical units. This expression will be valid in the range 5 - 60 solar radii; if we assume it to be approximately valid between the earth and Jupiter, the condition (2) for interplanetary diffraction becomes

$$r_o > 75\ R_{au}^2 \text{ kilometers.} \tag{7}$$

In view of the observed L-pulse correlation scale sizes of a few hundred kilometers, this condition appears to be satisfied along the line of sight between the earth and Jupiter. That is, the scale sizes and densities of electron inhomogeneities in the solar corona, when extrapolated to a few astronomical units, are consistent with the requirements for production of L-pulses by interplanetary diffraction.

VI. INTERPLANETARY DIFFRACTION AS THE SOURCE OF L-PULSES

a) Geometrical and Correlation Consideration

The geometry of the proposed L-pulse diffraction process is illustrated in Figure 7. In view of the high kinetic energy of the solar wind, radial motion with approximately constant velocity should be expected, even at several astronomical units. Irregularities moving radially outward from the sun with a constant velocity v_s have, perpendicular to the

line of sight, a velocity $v_s \sin \theta$ which reverses approximately at opposition. The magnitude of the projected velocity seen at the earth will be multiplied by a geometrical factor $(Z_1 + Z_2) / Z_2$ due to the finite distance of Jupiter; small aberration corrections for the orbital motion of earth and Jupiter are also appreciable. Except near opposition, the velocity will be roughly along the projection of the ecliptic on the plane perpendicular to the line of sight. Near opposition, the angle between the orbital planes of earth and Jupiter becomes comparable with θ, and the small projected velocities will take on a range of directions. Furthermore, small random velocity components may become important, obscuring the systematic behavior of the projected velocity near opposition.

Excluding the few days around opposition, this model makes an unambiguous prediction of a reversal in the sense of drift at aberration-corrected opposition. Such a correlation between the senseof time delay and the date with respect to opposition would produce two other spurious correlations. First, a correlation with civil date must be present if observations from only one apparition are available, but should vanish when roughly uniform numbers of events from all phases of a full orbital revolution of Jupiter become available. There must also be a correlation with local time, since meridian-centered observations before opposition are made in the early morning hours and those after opposition in the evening hours.

Figure 8 shows the time delay as a function of date from opposition for the 79 storms observed. The data plotted cover four apparations during which the date of opposition moved from 25 July (1961) to 13 November (1964).

The correlation is striking; only two reliability 2 and three reliability 3 points are in the wrong-delay sense. In addition, some tendency for the long delays to occur near opposition is seen, as would be expected from the geometry of Figure 7. The point at which delays reverse sign is slightly (~ 1 week) past opposition, in agreement with aberration predictions and specifically consistent with mean solar wind velocity of about 350 km/sec in the scintillating regions between earth and Jupiter.

Figure 9 presents the time delays as a function of date. The correlation follows from the fact that we are sampling only a third of Jupiter's orbital period. Thus, observations in January, where all delays are positive, always occurred after opposition; observations in June, where all delays are negative, always occurred before opposition. On the other hand April and September have been both pre- and post opposition months during the period 1961 - 1965; their delays are seen to be mixed. The apparent correlation with date is thus seen to be an artifact of the basic correlation with date from opposition.

In Figure 10, giving delay as a function of local time, correlation is again evident. However, all the points falling before 2100 prove to be data obtained after opposition; the points falling after 0300 were all obtained before opposition. Of the 18 points between 2100 and 0300, 6 are in violation of the local time correlation; this portion of the diagram shows no evidence of local time correlation. It is in this portion that pre- and post- opposition data are mixed; we therefore conclude that the local time correlation is also the expected consequence of the fundamental correlation with respect to opposition.

Figure 11 shows time delays as a function of local hour angle; no significant correlation is present except for the clustering of observations between -3^h and $+3^h$ as a result of observational procedures.

The time delays are thus seen to be associated with date from opposition in the predicted sense. The fact that they display no (unexpected) correlations with season, local time and local hour angle of observation is a further indication that the time-delayed L-pulses have no significant ionospheric component.

Two-station observations cannot furnish an observed direction of the drift velocity vector. However, the geometry of Figure 7 requires the systematic velocity to be parallel to the ecliptic, except near opposition when the difference between the orbital planes of the earth and Jupiter become important. For each observation in Table 4, the Pomfret and Bethany locations have been projected on a plane perpendicular to the line of sight to Jupiter, and the angle between the Bethany - Pomfret projection and the ecliptic calculated. Through a fortunate combination of geometric circumstances, the angle was quite small for a majority of the observations, permitting calculation of the velocity of the isophotal pattern without knowledge of the shape and orientation of its spatial correlation function.

Table 5

Table 5 summarizes the derived pattern velocities v_p for those dates where the velocity error is less than 33%. The starred dates are uncertain due to a large angle between the ecliptic and the Bethany - Pomfret line;

they are correct if the correlation function is either circularly symmetric or elliptical with major or minor axis along the ecliptic. Observations within 20 days of opposition have been omitted; the assumption that the projected solar wind velocity is parallel to the ecliptic will be bad in that region.

The pattern velocities are seen to be comparable with solar wind velocities, and to be systematically smaller near opposition where the component of the solar wind perpendicular to the line of sight grows small.

Those observations in Table 5 which have been analyzed by correlation techniques yield a value of the correlation scale X_o of the pattern along the ecliptic; values of X_o are seen to lie between about 150 and 1000 kilometers. The inhomogeneity scale in the diffracting medium must be of this order of magnitude or greater; such inhomogeneity scale sizes are consistent with limits set by coronal occultation observations.

We conclude that the general properties of L-pulses in Jupiter's decametric emission may be entirely explained by diffraction in the interplanetary medium.

b) Scale and Velocity of Inhomogeneities

Details of diffraction phenomena responsible for the L-pulses are not susceptible to simple treatment. The earth and Jupiter are imbedded in the diffracting medium, and the number density, electron excess, scale size and perpendicular velocity component of the inhomogeneities may each vary along the line of sight. Also, as noted earlier, since Jupiter is at a finite distance the diffraction pattern scale and velocity produced by inhomogeneites at distance Z_1 will be magnified by

$\frac{Z_2 + Z_1}{Z_2}$ (Figure 7; Ratcliffe 1956) over the pattern for a source at infinity.

Nevertheless, some further qualitative insight may be gained from arguments based on simple diffraction theory. To produce the fluctuations observed, an equivalent diffraction screen with $\Phi_o \sim 1$ radian and electron density correlation scale size r_o must be at a distance Z_1 such that

$$\frac{Z_1 Z_2}{Z_1 + Z_2} > \frac{r_o^2}{\lambda} \tag{8}$$

When $\Phi_o > 1$, arguments based on the focal distance of lenses (Mercier 1962) suggest that the appropriate form for the inequality is

$$\frac{Z_1 Z_2}{Z_1 + Z_2} > \frac{r_o^2}{\Phi_o \lambda} \tag{9}$$

When $\Phi_o \sim 1$, $r_o \approx X_o \frac{Z_2}{Z_1 + Z_2}$, where X_o is the observed correlation scale size of the fluctuations, and for $\Phi_o > 1$, $r_o \approx X_o \Phi_o \frac{Z_2}{Z_1 = Z_2}$.

Using these approximations in (9), we have

$$Z_1 > \frac{d \Phi_o \frac{X_o^2}{\lambda}}{d + \Phi_o \frac{X_o^2}{\lambda}} \tag{10}$$

where $d = Z_1 + Z_2$ is the distance from earth to Jupiter.

For $X_o = 500$ km, (10) requires $Z_1 > 1.85\ (10)^7$ km for $\Phi_o \sim 1$ and $Z_1 > 1.85\ (10)^8$ km = 1.23 a.u. for $\Phi_o \sim 10$. Thus, inhomogeneities closer than a few

tenths of an astronomical unit should not contribute appreciably to the pattern.

Two lines of argument suggest that inhomogeneities near Jupiter will not contribute. First, if one makes the plausible assumption that $\frac{r_o^2}{\Phi_o}$ does not decrease along the line of sight, inhomogeneities within a few tenths of an astronomical unit of Jupiter will produce correlation scale sizes at the earth an order of magnitude larger than the same inhomogeneities roughly half-way between the earth and Jupiter. The L-pulses studied are the smallest scale structure in most records; they are therefore not produced by inhomogeneities near Jupiter unless no other inhomogeneities of similar or smaller size exist along the line of sight.

A second line of argument is based on the apparent time stability of the drifting isophotal pattern. Due to the magnification of the drift velocity by $\frac{Z_1 + Z_2}{Z_2}$, clouds near Jupiter will produce high and variable velocity projections which will cause the diffraction pattern to change rapidly as it drifts. On the other hand, clouds between 1 and 3 au away from the earth have a nearly constant projected velocity, since $\sin \theta$ and $\frac{Z_1 + Z_2}{Z_2}$ are changing in opposite directions.

Thus, values of r_o between a few hundred and few thousand kilometers are consistent with the observations, with most of the diffraction occuring over a path of about 2 astronomical units, centered half-way between the earth and Jupiter.

The angular diameter β of the inhomogeneities is quite small:

$$\beta = \frac{X_o \Phi_o Z_2}{Z_1 (Z_1 + Z_2)} \qquad (11)$$

The maximum angular scale of inhomogeneities producing fluctuation occurs when Z_1 is as small as it can get and still satisfy (10). Using (10) in (11), we obtain

$$\beta_{max} \gtrsim \frac{\lambda}{X_o} \quad \text{radian} \qquad (12)$$

This is an observable quantity; for X_o = 500km, β_{max} = 5".5. The angular scale of the source on Jupiter must be substantially smaller than this value; high fluctuation indices would otherwise be impossible. The failure of Cyg A and Cas A to exhibit L-pulses is a result of their angular scale being much greater than β_{max}.

Slee and Higgins (1966) have reported an important series of measurements of the apparent diameter of Jupiter's decametric emission source, using baselines up to 200km in length at 19.7 Mc/s. Convincing evidence of an apparent source angular size on the order of 10 to 15 seconds of arc, together with apparent fluctuations in size, was interpreted as a result of interplanetary diffraction. To compare these observations with the results of the present paper, it should be noted that the apparent angular scale produced in a point source at distance $Z_1 + Z_2$ by a diffracting medium at distance Z_1 will be $\alpha_o' = \alpha_o \frac{Z_2}{Z_1+Z_2}$. Using (4) and taking $X_o = \phi_o X_o \frac{Z_2}{Z_1+Z_2}$, we have $\alpha_o' = \lambda/\pi X_o$. The angular sizes quoted by Slee and Higgins refer to the width to half-power of an equivalent gaussian distribution; the parameter α_o' used in this paper is the half-width to 1/e of an equivalent gaussian distribution. Thus, Slee and Higgins' range of ten to fifteen seconds of arc corresponds to a range in α_o' of 6 to 9 seconds of arc at 19.7 Mc/s, or for $\phi_o > 1$ and 22.2 Mc/s, a range in α_o' of 4.7 to 7 seconds of arc. Expected values of α_o' based on our data are tabulated in Table 5, and are seen

to be about a factor of two smaller than indicated by the observations of Slee and Higgins.

Agreement between an observed angular scale and an angular scale predicted from an observed amplitude correlation scale is to be expected only if the amplitude and phase scintillations arise in the same region between earth and Jupiter, or in different regions having the same value of $\chi_0 = \frac{r_0}{\phi_0} \frac{z_1+z_2}{z_2}$. Arguments in the previous section suggest that the irregularities responsible for amplitude scintillation are in a broad region half-way between the earth and Jupiter; none of these arguments apply to the irregularities responsible for phase scintillation. Indeed, one would expect contributions from all along the line of sight; however the apparent angular scale α_0' would be primarily determined by that significantly contributing region which is characterized by the smallest value of $\frac{r_0}{\phi_0} \frac{z_1+z_2}{z_2}$. Thus, among other possibilities, the amplitude and angular size data are consistent (Slee, private communication) with production of amplitude scintillation by irregularities about half-way to Jupiter $\left(\frac{z_1+z_2}{z_2} x_2\right)$, and production of phase fluctuation by irregularities near the earth $\left(\frac{z_1+z_2}{z_2} x_1\right)$, with r_0/ϕ_0 remaining approximately constant over the line of sight. These near-by irregularities do not appear in the amplitude data since (10) is not satisfied.

Time delays of L-pulses between their spaced receiver sites were also noted by Slee and Higgins; their observations appear to be consistent with the results of the present paper when the rather steep inclination of their baseline to the ecliptic is taken into account.

c) Interplanetary Scintillation of Discrete Radio Sources

The flux from discrete sources of small angular diameter has been

shown to fluctuate with a time scale of seconds (see e.g. Hewish et al. 1964). Extrapolating results of observation of solar occultations of Taurus A, these authors proposed an interplanetary diffraction mechanism with $\alpha_o \approx 1''$ at 178 Mc/s and $\Phi_o > 1$. Their figures apply at 0.5 a.u.; extrapolating to 2 a.u. and multiplying by the square of the wavelength ratio, we obtain $\alpha_o = 16''$, and $\alpha_o' = 8''$ as the expected value for the region of the interplanetary medium which produces Jupiter L-pulses. This value is about a factor of 3 larger than the results of the present paper (see Table 5). The discrepancy probably lies in the interpretation by Hewish, et al, that $\Phi_o > 1$ at 178 Mc/s (1.7 meters). In fact, in a more recent paper Hewish, Dennison, and Pilkington (1966) report spaced-receiver observation of 3.7 meter interplanetary scintillation of the quasi-stellar source 3C48. Time delays between receivers were observed, and evidence that $\Phi_o < 1$ at 3.7 meters was presented, suggesting that an average electron inhomogeneity scale size of about 150km was present along the lines of sight used during the observation. The fact that $\Phi_o < 1$ above 3.7 meters removes the discrepancy between Hewish's earlier work and the present paper, and suggests that at 22.2 Mc/s (13.5 meters), $\Phi_o \approx 1$.

The simple diffraction geometry presented in this paper is thus consistent with Slee's observations of Jupiter's apparent decametric angular size and with the interplanetary scintillation observations of Hewish, and in addition explains the observed behavior of L-pulses.

Three-station observation of L-pulse obtained in 1965 and 1966 are now being reduced, and will be capable of establishing observationally the average shape and velocity vector of the scattering inhomogeneities. It is important to remark that, for the wavelength and line of sight used,

θ_{max} is determined directly by the spaced-receiver observations, subject only to the uncertain validity of the simple diffraction theor on which the result is based. Thus, spaced-receiver observations of Jupiter and, more importantly, of discrete radio sources can provide a calibration for the use of interplanetary scintillation as an angular-diameter measuring technique. It may also be possible by observations of this type, using Jupiter as a source, to detect the presence of the transition region in the solar wind should it ever lie within the orbit of Jupiter.

The authors would like to express their thanks for the assistance of Mr. J. R. McCullough and the Pomfret School, Dr. F. R. Zabriskie of Van Vleck Observatory, and Dr. K. L. Franklin of the American Museum - Hayden Planetarium in establishing and running the spaced receivers, and for the assistance of Mr. Alfred Kelleher of the Research Corporation in setting up the initial spaced-receiver system in 1958. Particular thanks are due Mr. James B. Didriksen of the Yale Observatory who was responsible for the bulk of the data reduction. We would also like to thank Mr. O. B. Slee of the Royal Radar Establishment, Malvern, England, who pointed out an error in an earlier version of this paper.

This program was undertaken with the aid of grants from the Research Corporation, and was primarily supported by grants from the National Science Foundation (GP 4086) and the National Aeronautics and Space Administration (NsG 407) to Yale University; the bulk of the work was accomplished while the authors were with the Yale Observatory.

REFERENCES

Bigg, C. H., 1964, Nature, 203, 1008.

Briggs, B. H. and Parkin, I. A., 1963 Jour. Atm. and Terr. Phys., 25, 339.

Carr, T. D., Brown, G. W., Smith, A. G., Higgins, C. S., Bollhagen, H., May, J., and Levy, J., 1964, Ap. J., 140, 778.

Carr, T. D., Smith, A. G., Bollhagen, H., Six, N. F., and Chatterton, N. E., 1961, Ap. J., 134, 105.

Douglas, J. N., 1960, Ph.D. Dissertation, Yale University, New Haven, Conn.

_____. 1963, Trans. Amer. Geophys. Union, 44, 887 (Abstract).

_____. 1964, IEEE Trans. Antennas and Propagation, AP-12, 839.

Douglas, J. N. and Smith, H. J., 1961, Nature, 192, 741.

_____. 1963a, Mem. Soc. Roy. Sci. Liege., 7, 543.

_____. 1963b, A. J., 68, 163.

_____. 1963c, Nature, 199, 1080.

Erickson, W. C., 1964, Ap. J., 139, 1290.

Gallet, R., 1961, Planets and Satellites, ed. G. P. Kuiper and B. M. Middlehurst (Chicago: Univ. of Chicago Press), chap. 14.

Gardner, F. F. and Shain, C. A., 1958, Australian J. Phys., 11, 55.

Hewish, A., 1955, Proc. Roy. Soc. London A, 228, 238.

_____. 1958, M. N., 118, 534.

Hewish, A., Dennison, P. A., and Pilkington, J. D. H., 1966, Nature, 209, 1188.

Hewish, A. and Wyndham, J. D., 1963, M. N., 126, 469.

Hewish, A., Scott, P. F., and Wills, D., 1964, Nature, 203, 1214.

Mercier, R. P., 1962, Proc. Camb. Phil. Soc., 58, 382.

Neugebauer, M. and Snyder, C. W., 1965, J. G. R., 70, 1587.

Phillip, K. W., 1957, A. J., 62, 145 (Abstract).

Ratcliffe, J. A., 1956, Reports on Progress in Physics, 19, 188.

Slee, O. B. and Higgins, C. S., 1966, Australian J. Phys., 19, 167.

Slee, O. B., 1961, M. N., 123, 223.

Smith, A. G., Carr, T. D., and Six, N. F., 1963, Mem. Soc. Roy. Sci. Liege, 7, 543.

Smith, H. J. and Douglas, J. N., 1959, in Paris Symp. on Radio Astronomy (Stanford: Stanford Univ. Press), p. 53.

_____. 1962, A. J., 67, 120 (Abstract).

Smith, H. J., Lasker, B. M., and Douglas, J. N., 1960, A. J., 65, 487 (Abstract).

Snyder, C. W., Neugebauer, M., and Rao, V. R., 1963, J. G. R., 68, 6361.

Vitkevitch, V. V., 1960, Soviet Astr.-A. J., 4, 31.

_____. 1961, Soviet Astr.-A. J., 4, 897.

Warwick, J. W., 1961, Ann. N. Y. Acad. Sci., 95, 39.

_____. 1963, Ap. J., 137, 41.

FIGURE CAPTIONS

Figure 1 - Hourly average 22.2 Mc/s flux from Jupiter during September, 1964. Abscissa is relative flux; the highest values are approximately 7 times the 22.2 Mc/s flux from Cygnus A. Note activity periods ending around 7 September and beginning around 13 September; minima around September 23 and 28 may also be real.

Figure 2 - Portion of 22.2 Mc/s Jupiter storm of 20 January 1965. The burst groups at Pomfret and Bethany gradually drift in and out of correlation due to ionospheric scintillation. The burst group at 1734 EST appears at high speed in Figure 3.

Figure 3 - High speed record of burst group on 20 January 1965 obtained at 0.2 inch/second with time constant of 10 milliseconds. The burst group is resolved into L-pulses; the Pomfret trace is similar to the Bethany trace, but lags 0.3 seconds behind it.

Figure 4 - One inch per second record of a 22.2 Mc/s Jupiter storm on 18 July 1961, showing S-pulses superimposed on L-pulses. No time delays are evident in this nearly perfectly correlated record.

Figure 5 - Tracing of high-speed multifrequency records of a frequency drifting burst group on 29 March 1960. Note the simultaneity of the L-pulses when present, irrespective of amplitude.

Figure 6 - Delay histograms for 30 April 1961.

Figure 7 - Proposed diffraction geometry, showing reversal of sense of drift near opposition.

Figure 8 - Plot of time delays versus date from opposition including data from four oppositions. A positive delay means Pomfret lags Bethany, and is seen to be characteristic of observations after opposition.

Figure 9 - Plot of time delay versus date. Note the failure of correlation in April and September, months which were both pre- and post-opposition during 1961 - 1965.

Figure 10 - Plot of time delay versus local time. Note the failure of correlation between 2100 and 0300, the only hours of the day when both pre- and post-opposition observations are available.

Figure 11 - Plot of time delay versus local hour angle, showing the clustering of observations between + 3^h and - 3^h but no other correlation.

Table 1. CLASSIFICATION OF JOVIAN NOISE STORM ACTIVITY

Type	Duration	Principal Cause
Activity Periods	Days to Weeks	Beating of rotation periods of earth and Jupiter and revolution period of Io; intrinsic variation of source activity may also be present.
Noise Storms	Minutes to Hours	Rotating directive emitter and receiver.
Burst Groups	Seconds to Minutes	Ionospheric scintillation, modulating a source already having some fluctuation on this scale.
L-Pulses	0.1 to 5 Seconds	Interplanetary scintillation (this paper)
S-Pulses	<0.01 to 0.1 Seconds	Obscure

Table 2

Station	Longitude (W)	Latitude (N)	Altitude (Meters)	Azimuth	Distance(km)
Bethany	72°59!0	41°25!6	189	----	----
Hendrie	72°55!5	41°18!6	25	159°47!3	13.857
Middletown	72°39!6	41°33!1	75	63°48!6	31.113
Pomfret	71°58!0	41°53!0	170	59°10!9	98.737
Huntington	73°20!2	40°49!3	76	204°21!8	73.509

Table 3

Year	Stations and Receivers in Operation
1960	Bethany: 21.60, 21.83, 22.08 and 22.28 Mc/s
1961	Bethany: 22.20 Mc/s; Hendrie 22.20 Mc/s; Middletown: 22.20 Mc/s; Pomfret: 22.20 Mc/s
1962,1963	Bethany: 22.20 Mc/s; Pomfret: 22.20 Mc/s
1964	Bethany: 21.9, 22.20, 22.25, 22.60 Mc/s; Pomfret: 22.20 Mc/s
1965	Bethany: 21.90, 22.20, 22.25, 22.60 Mc/s; Pomfret: 22.20 Mc/s; Huntington: 22.20 Mc/s.

TABLE 4

Summary of Time Delay Observations

Date		Days Since Opposition	EST	Hour Angle	Delay* (sec) Pomfret - Bethany	Reliability†
1961						
April	16	-100	0325	-0315	-0.25 ±.05	2
	18	- 98	0500	-0136	-0.20 ±.05	2
	30	- 86	0423	-0130	-0.30 ±.10	2
July	18	- 7	0330	+0259	0.00 ±.01	1
1962						
June	6	- 86	0430	-0120	-0.03	3
	8	- 84	0300	-0242	-0.15 ±.05	2
	11	- 81	0400	-0130	-0.09	3
	23	- 69	0310	-0135	-0.15 ±.04	2
	25	- 67	0430	-0008	-0.15	3
	28	- 64	0400	-0026	-0.10	3
	30	- 62	0330	-0048	-0.08 ±.03	2
July	27	- 35	0140	-0048	+0.37	3
	30	- 32	0010	-0206	-0.10	3
	31	- 31	0420	+0209	-0.02	3
Aug.	1	- 30	0030	-0138	-0.10	3
	17	- 14	2300	-0159	-0.02	3
	22	- 9	2230	-0206	-0.44 ±.10	3
	29	- 2	2250	-0112	-0.6 ±.10	2
Sept.	16	+ 16	2345	+0104	+0.75	3
	20	+ 20	2025	-0159	-0.2	3
		+ 20	2210	-0014	+0.1	3
	22	+ 22	2200	-0016	+0.53 ±.08	2
	25	+ 25	1930	-0233	+0.35 ±.05	1
		+ 25	2030	-0133	+0.33 ±.08	2
Oct.	9	+ 39	2031	-0032	+0.17 ±.04	2
	24	+ 54	2101	+0100	+0.30	3
	25	+ 55	2050	+0053	-0.01 ±.05	2
1963						
June	1	-129	1016	+0214	-0.06 ±.03	2
	11	- 89	0930	+0344	+0.05 ±.03	2
	28	- 72	0151	-0253	-0.08 ±.03	2
Sept.	25	- 13	2350	-0047	-0.15 ±.05	2
Oct.	20	+ 12	2233	-0014	+0.075±.03	2
	21	+ 13	2300	+0018	+0.075±.05	3
	29	+ 21	0032	+0221	+0.15	3

TABLE 4 Continued

Date		Days Since Opposition	EST	Hour Angle	Delay* (sec) Pomfret - Bethany	Reliability†
Nov.	1	+ 24	2052	-0103	+0.42 ±.03	1
	17	+ 40	2235	+0149	+0.32 ±.03	1
	18	+ 41	1928	-0114	+0.45 ±.08	2
	22	+ 45	1910	-0115	+0.25 ±.04	2
	29	+ 52	2030	+0030	+0.15 ±.05	2
Dec.	14	+ 67	1945	+0048	+0.25 ±.05	2
		+ 67	2030	+0138	+0.15 ±.05	2
1964						
Jan.	10	+ 94	1720	+0001	+0.13 ±.05	2
Feb.	8	+123	1430	-0112	+0.20	3
	11	+126	1426	-0106	+0.25 ±.04	2
June	4	-162	0840	-0101	-0.27 ±.04	1
	12	-154	0600	-0317	-0.04 ±.04	1
July	30	-106	0400	-0245	-0.23 ±.04	1
Sept.	30	- 44	0411	+0121	-0.13 ±.05	1
Nov.	17	+ 4	2120	-0157	+0.1 ±.1	3
Dec.	26	+ 43	1820	-0208	+0.10 ±.03	1
1965						
Jan.	10	+ 58	1710	-0217	+0.22 ±.05	3
		+ 58	1819	-0107	+0.22 ±.03	1
	20	+ 68	1604	-0244	+0.25 ±.04	1
		+ 68	1643	-0205	+0.30 ±.05	1
		+ 68	1727	-0121	+0.30 ±.04	1
	25	+ 73	2129	+0300	+0.2 ±.1	3
	27	+ 75	1740	-0042	+0.37 ±.04	1
	29	+ 77	1915	+0101	+0.30 ±.08	2
	31	+ 79	2011	+0204	+0.27 ±.05	1
Feb.	4	+ 83	1553	-0159	0.00 ±.05	1
	11	+ 90	1439	-0248	-0.05 ±.05	3
	13	+ 92	1617	-0103	+0.17 ±.04	2
	15	+ 94	1717	+0004	+0.15 ±.05	2
	18	+ 97	1527	-0136	+0.10 ±.05	2
	20	+ 99	1704	+0008	+0.20 ±.03	1
	25	+104	1608	-0031	+0.15 ±.1	3
March	7	+114	1600	-0006	0.00 ±.05	2
	20	+127	1949	+0425	+0.15 ±.1	3
	21	+128	1603	+0042	+0.07 ±.05	3
	23	+130	1539	+0025	+0.05 ±.05	3
	24	+131	1325	-0146	+0.10 ±.05	2
	26	+133	1600	+0055	+0.09 ±.03	2
	28	+135	1720	+0222	+0.20 ±.06	2
	29	+136	1135	-0320	+0.12 ±.06	2

TABLE 4 Continued

Date	Days Since Opposition	EST	Hour Angle	Delay* (sec) Pomfret - Bethany	Reliability†
April 3	+141	1231	-0209	+0.25 ±.03	1
21	+159	1550	+0205	+0.07 ±.03	2
24	+162	1044	-0251	+0.08 ±.05	3
30	+168	1110	-0207	+0.10 ±.06	3
May 8	+176	1654	+0400	-0.04 ±.02	2

* Delays are defined as the most frequent difference (Pomfred minus Bethany) in time of arrival of L-pulses, or as the time shift required for maximum cross-correlation between records.

† The reliability numbers are coded as follows:

Reliability	Definition
1	Unimodal delay histogram with well-defined narrow peak and more than 15 delay measurements, or a delay obtained from cross-correlation analyses.
2	Unimodal delay histogram with a broad peak.
3	Bimodal or very broad delay histogram, or too few measurements for 1 or 2.

Table 5

Date	Date from Opposition	V_p (km/sec)	X_o (km)	β_o max	α_o [1]
1961					
Apr 18	-98	490±120			
30	-86	320±105	420±150	6".6	2".1
1962					
Jun 8	-84	640±210			
23	-69	660±160			
Sep 22	+22	175±30			
25	+25	275±40			
25	+25	300±75			
Oct 9	+39	580±150			
1963					
Nov 1	+24	235±20	300±60	9".3	3".0
17	+40	230±25			
22	+45	395±70			
29	+52	590±200			
Dec 14	+67	350±200			
14	+67	490±160			
1964					
Feb 11	+126	400±70			
Jun 4	-162	360±50	180±50	15".3	4".6
Jul 30	-106	350±70			
Dec 26	+43	950±320	1190±500	2".3	".7
1965					
Jan 10	+58	430±110	590±250	4".7	1".5
10	+58	450±70			
20	+68	360±60	290±100	9".6	3".1
20	+68	320±55			
20	+68	330±50			
27	+75	265±30	250±60	11".1	3".5
29	+77	290±70			
31*	+79	240±50	140±50	20".0	6".4
Feb 13	+92	580±150	400±200	6".9	2".2
15	+94	630±210			
20	+97	470±70			
Mar 26*	133	950±320			
28*	135	312±100			
29	136	690±230			
Apr 3	141	380±50			

Figure 1

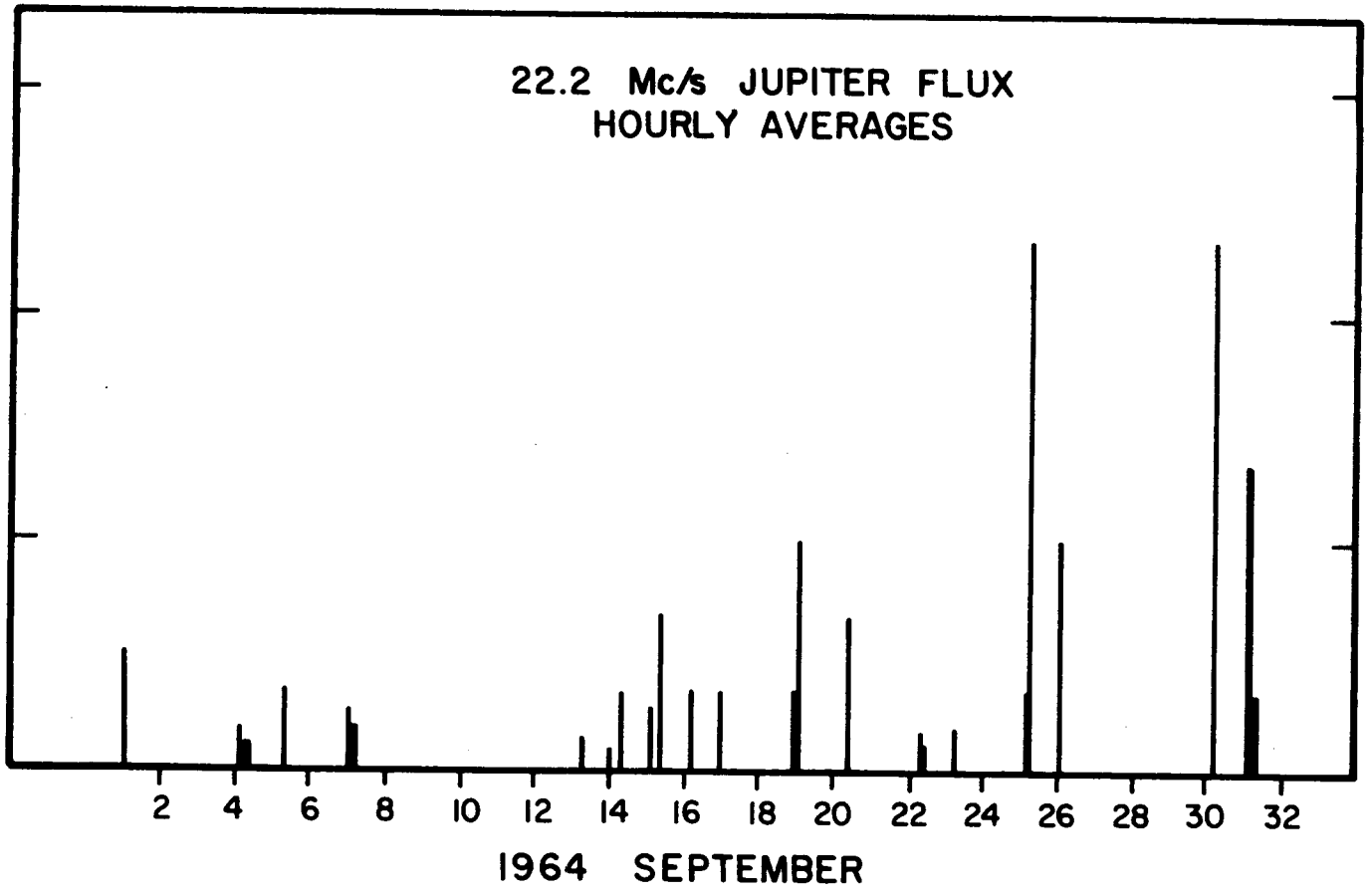
22.2 Mc/s JUPITER FLUX
HOURLY AVERAGES
2
4
6
8
10
12
14
16
18
20
22
24
26
28
30
32
1964 SEPTEMBER

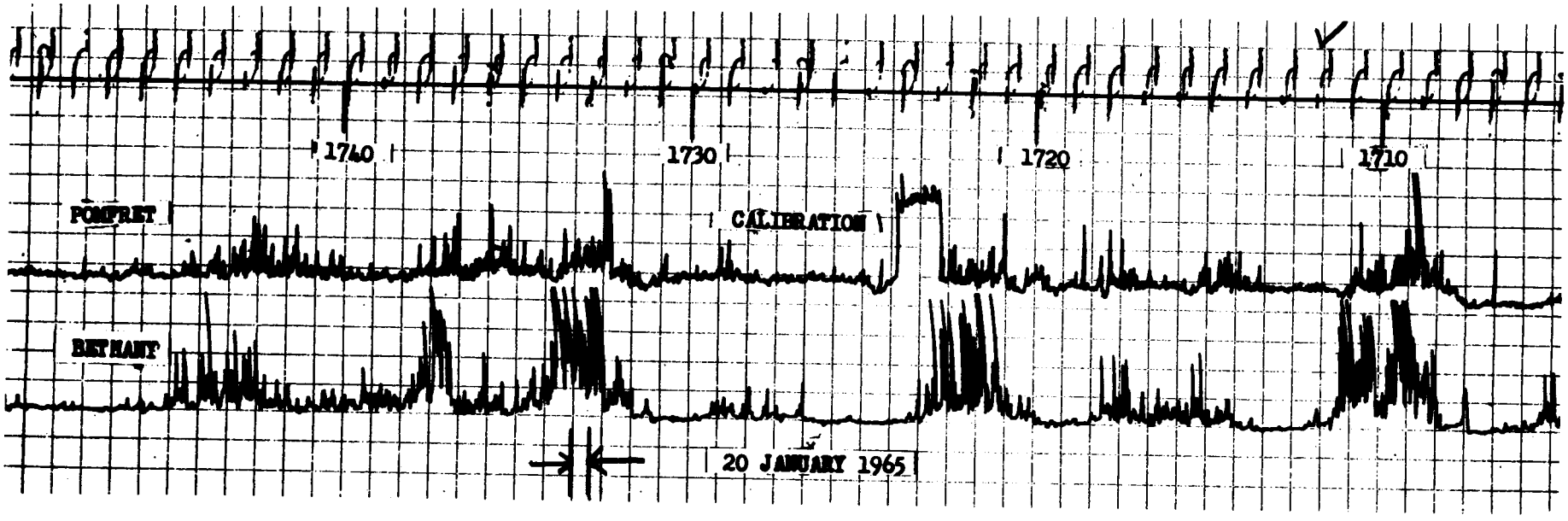
1740
1730
1720
1710
POMFRET
CALIBRATION
BETHANY
20 JANUARY 1965

FIGURE 2

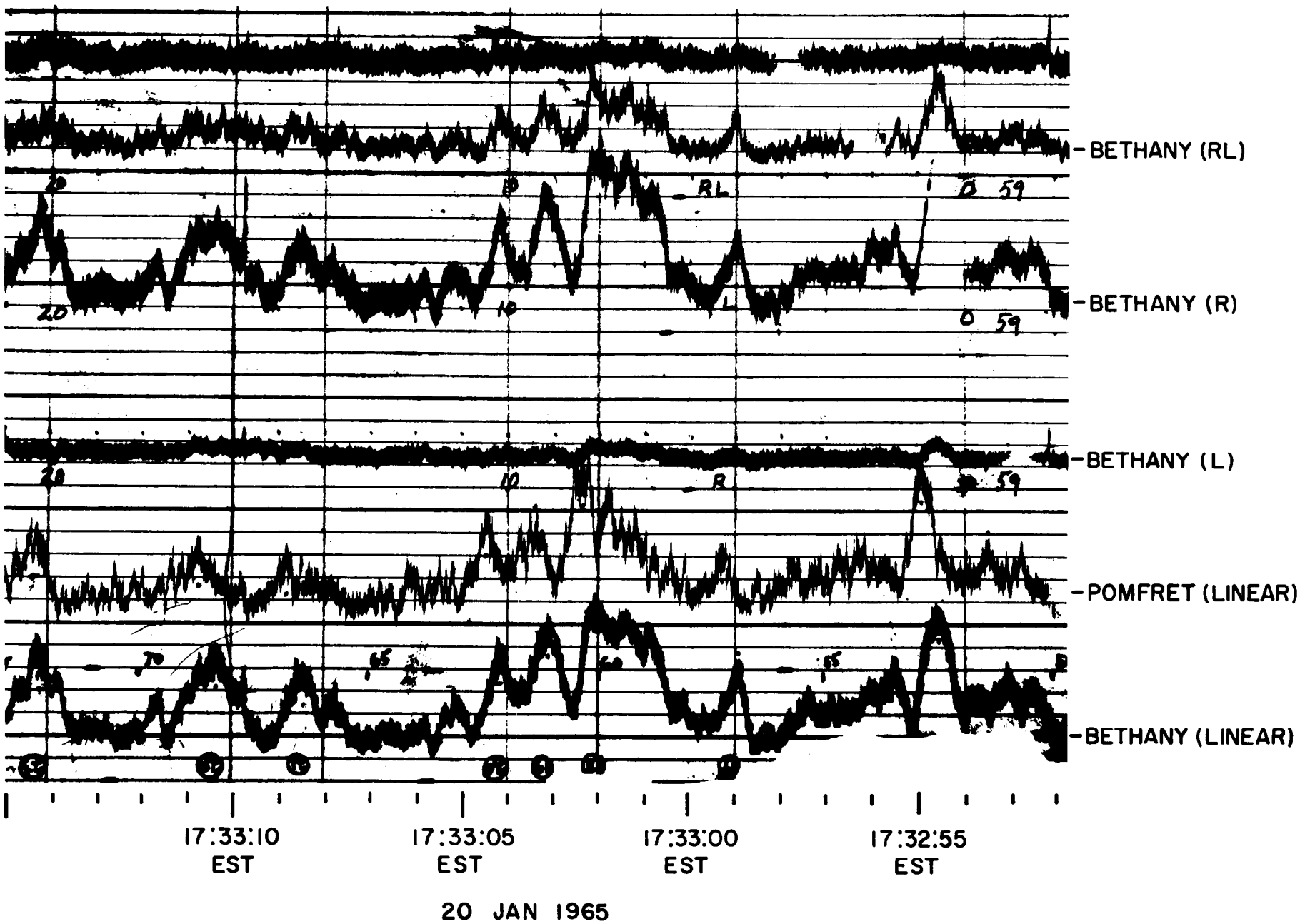
BETHANY (RL)
BETHANY (R)
BETHANY (L)
POMFRET (LINEAR)
BETHANY (LINEAR)
17:33:10 EST
17:33:05 EST
17:33:00 EST
17:32:55 EST
20 JAN 1965

FIGURE 3

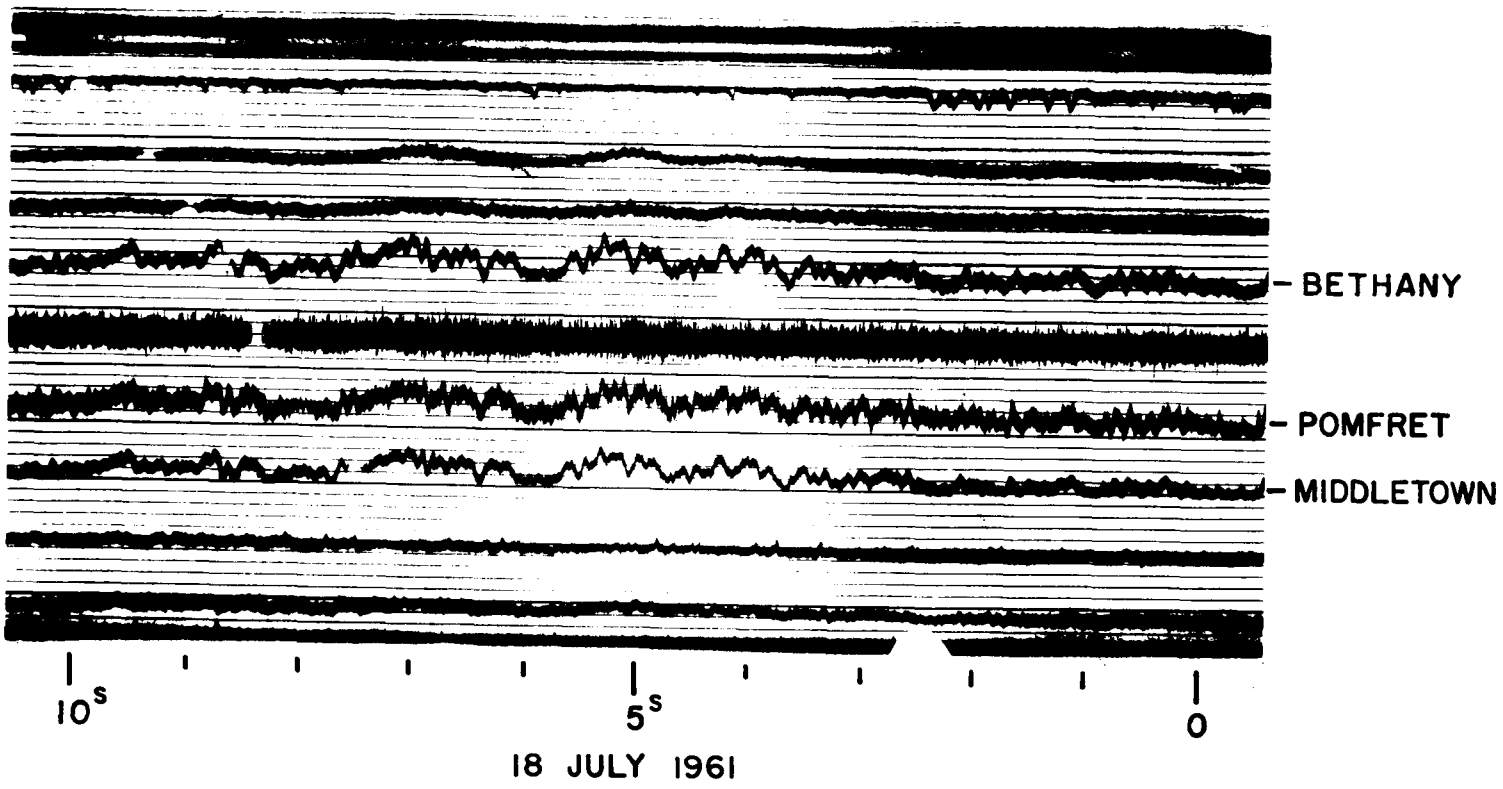

FIGURE 4

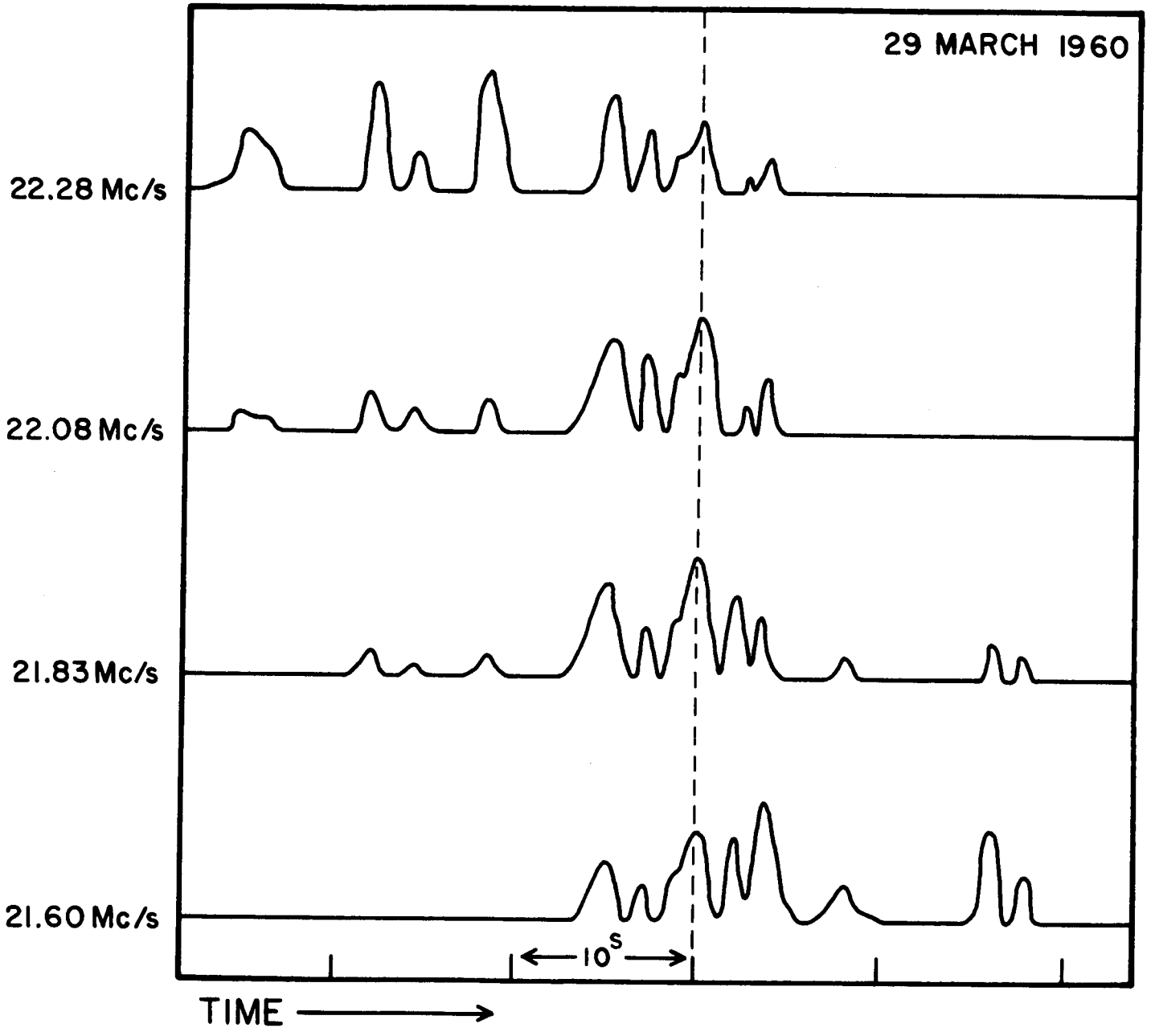
29 MARCH 1960
22.28 Mc/s
22.08 Mc/s
21.83 Mc/s
21.60 Mc/s
10^s
TIME

Figure 6

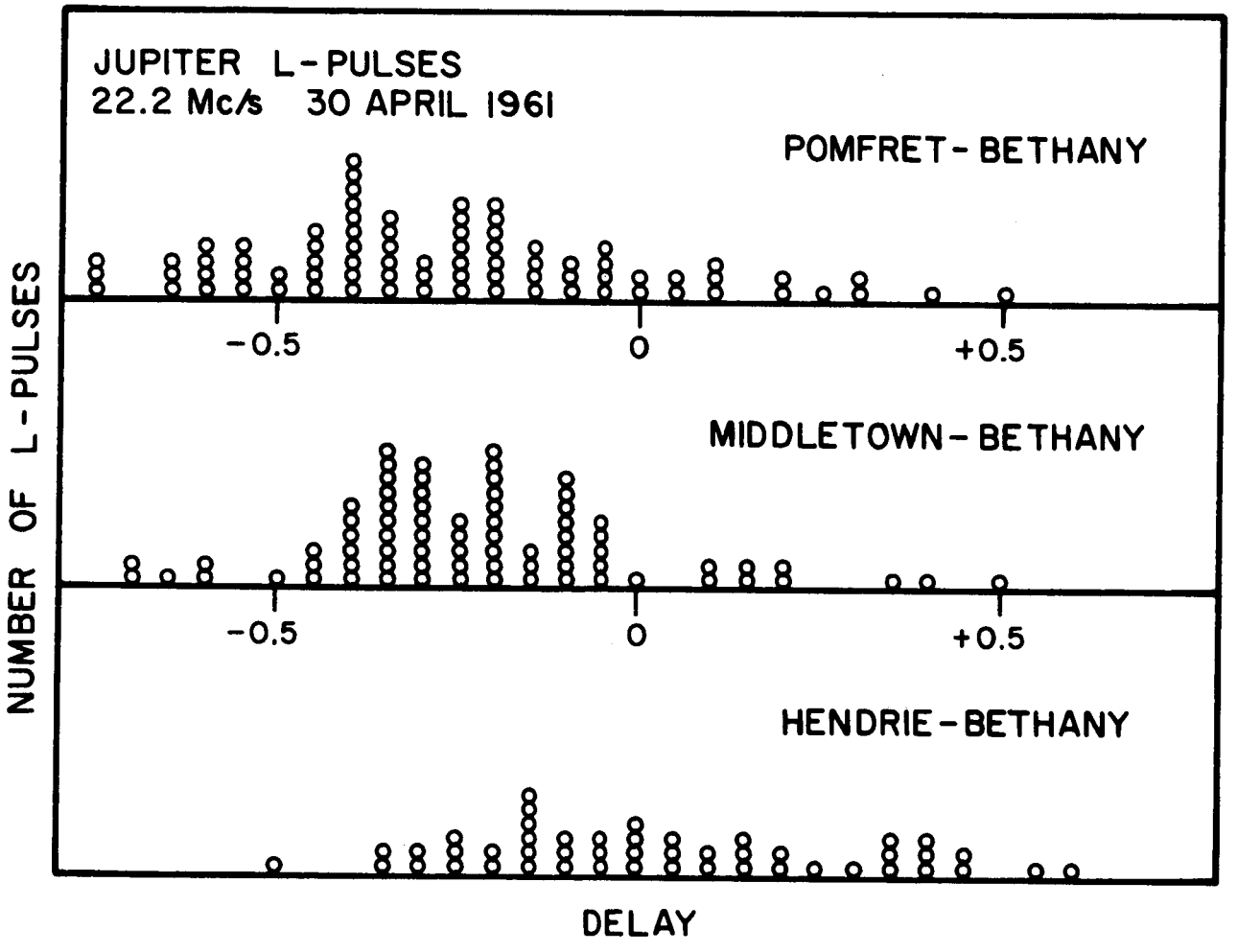
JUPITER L-PULSES
22.2 Mc/s 30 APRIL 1961
POMFRET-BETHANY
-0.5
0
+0.5
MIDDLETOWN-BETHANY
-0.5
0
+0.5
HENDRIE-BETHANY
NUMBER OF L-PULSES
DELAY

Figure 7

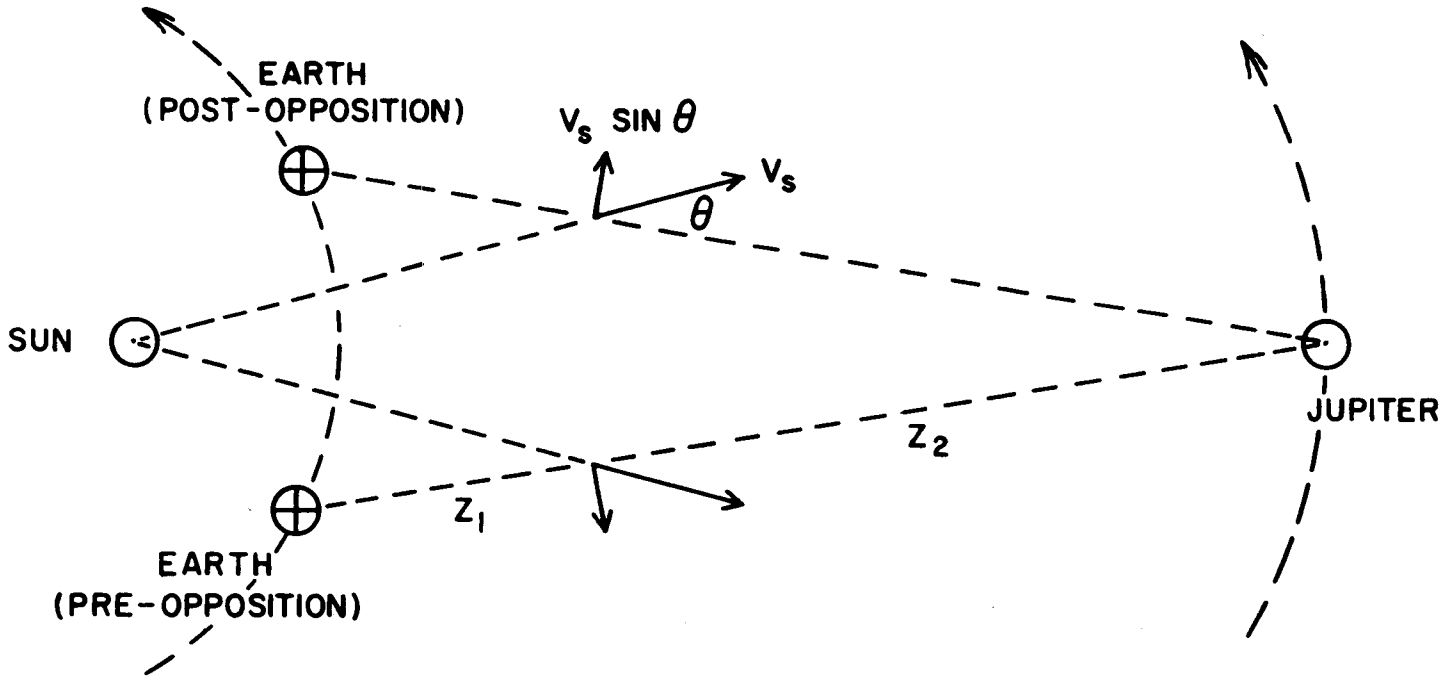
EARTH
(POST-OPPOSITION)
V_s SIN θ
V_s
θ
SUN
JUPITER
Z_2
Z_1
EARTH
(PRE-OPPOSITION)

Figure 5

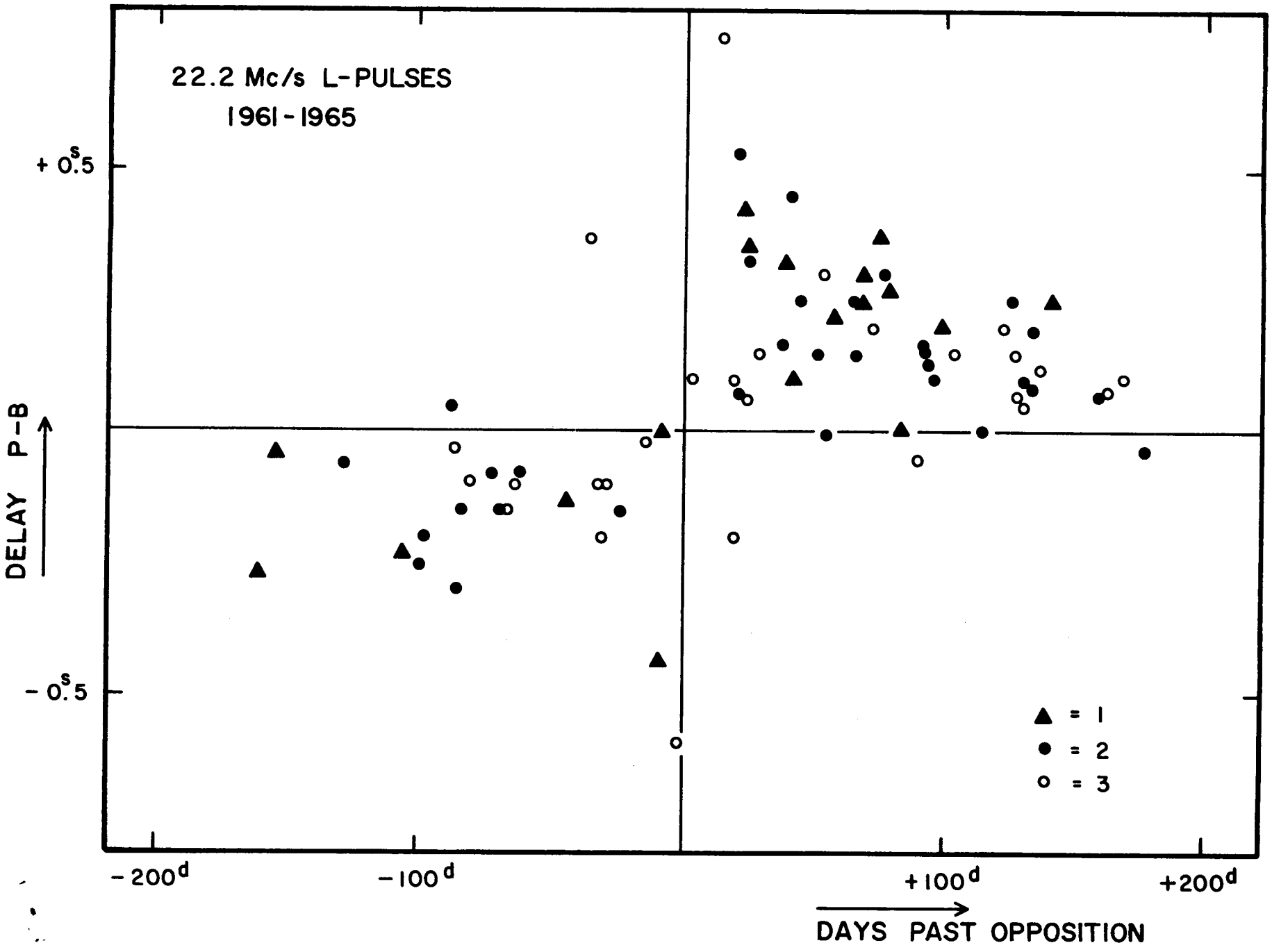
22.2 Mc/s L-PULSES
1961-1965
+ 0.s5
- 0.s5
DELAY P-B
▲ = 1
● = 2
○ = 3
-200d
-100d
+100d
+200d
DAYS PAST OPPOSITION

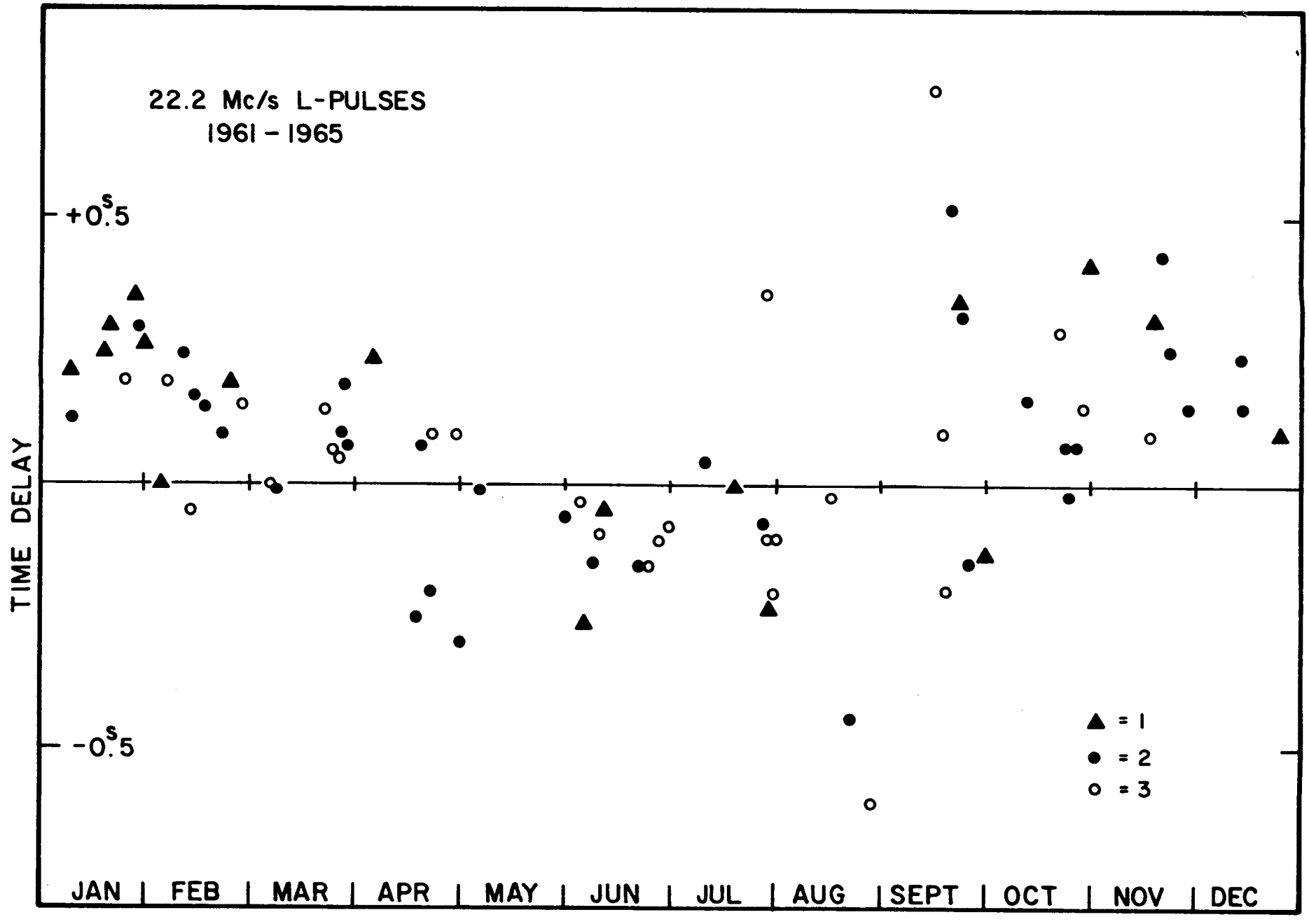
22.2 Mc/s L-PULSES
1961 - 1965
+0.5
-0.5
TIME DELAY
▲ = 1
● = 2
○ = 3
JAN
FEB
MAR
APR
MAY
JUN
JUL
AUG
SEPT
OCT
NOV
DEC

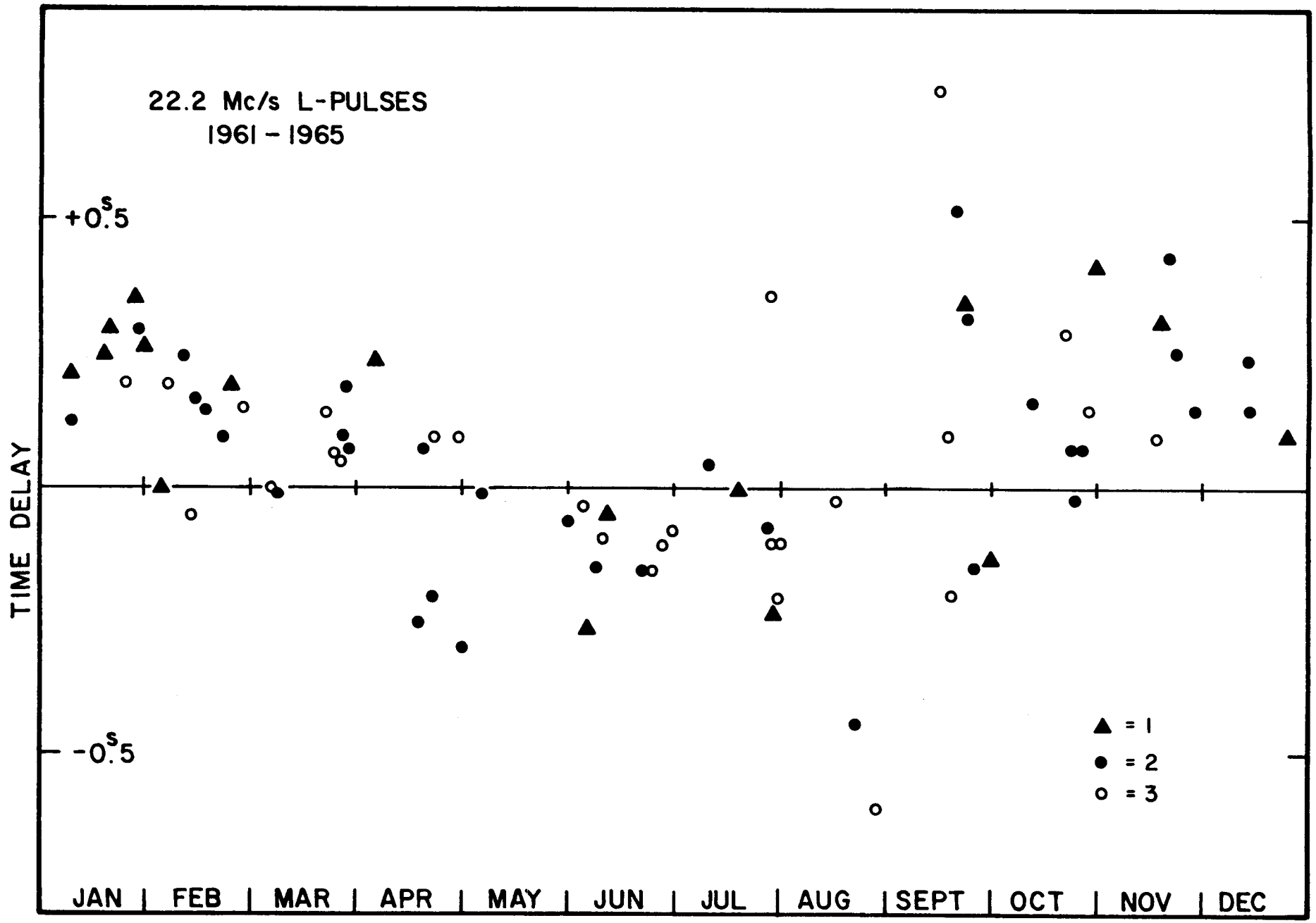
22.2 Mc/s L-PULSES
1961 - 1965
+0.5
-0.5
TIME DELAY
▲ = 1
● = 2
○ = 3
JAN
FEB
MAR
APR
MAY
JUN
JUL
AUG
SEPT
OCT
NOV
DEC

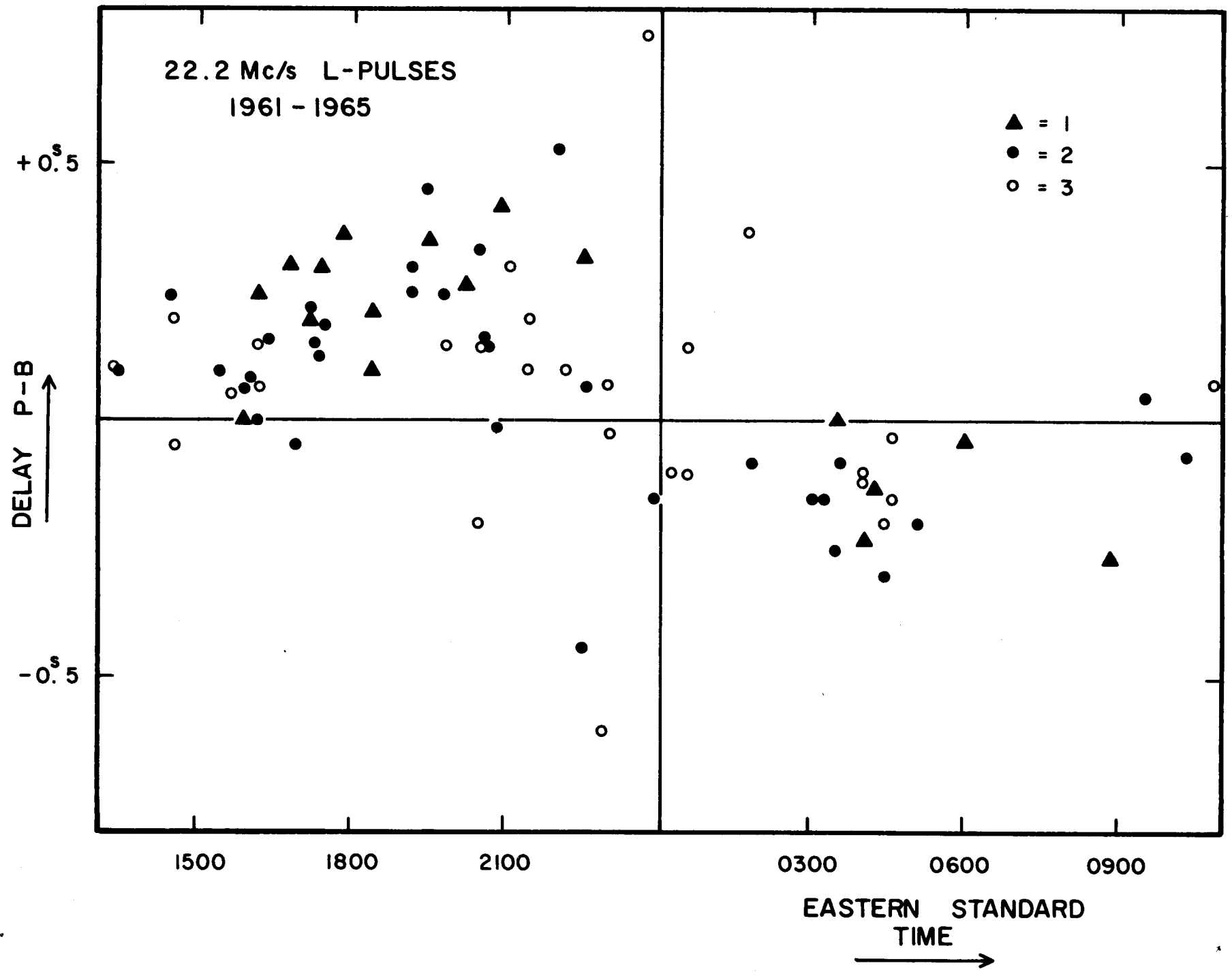
22.2 Mc/s L-PULSES
1961 - 1965
▲ = 1
● = 2
○ = 3
+0.s5
-0.s5
DELAY P-B
1500
1800
2100
0300
0600
0900
EASTERN STANDARD TIME

Figure 11

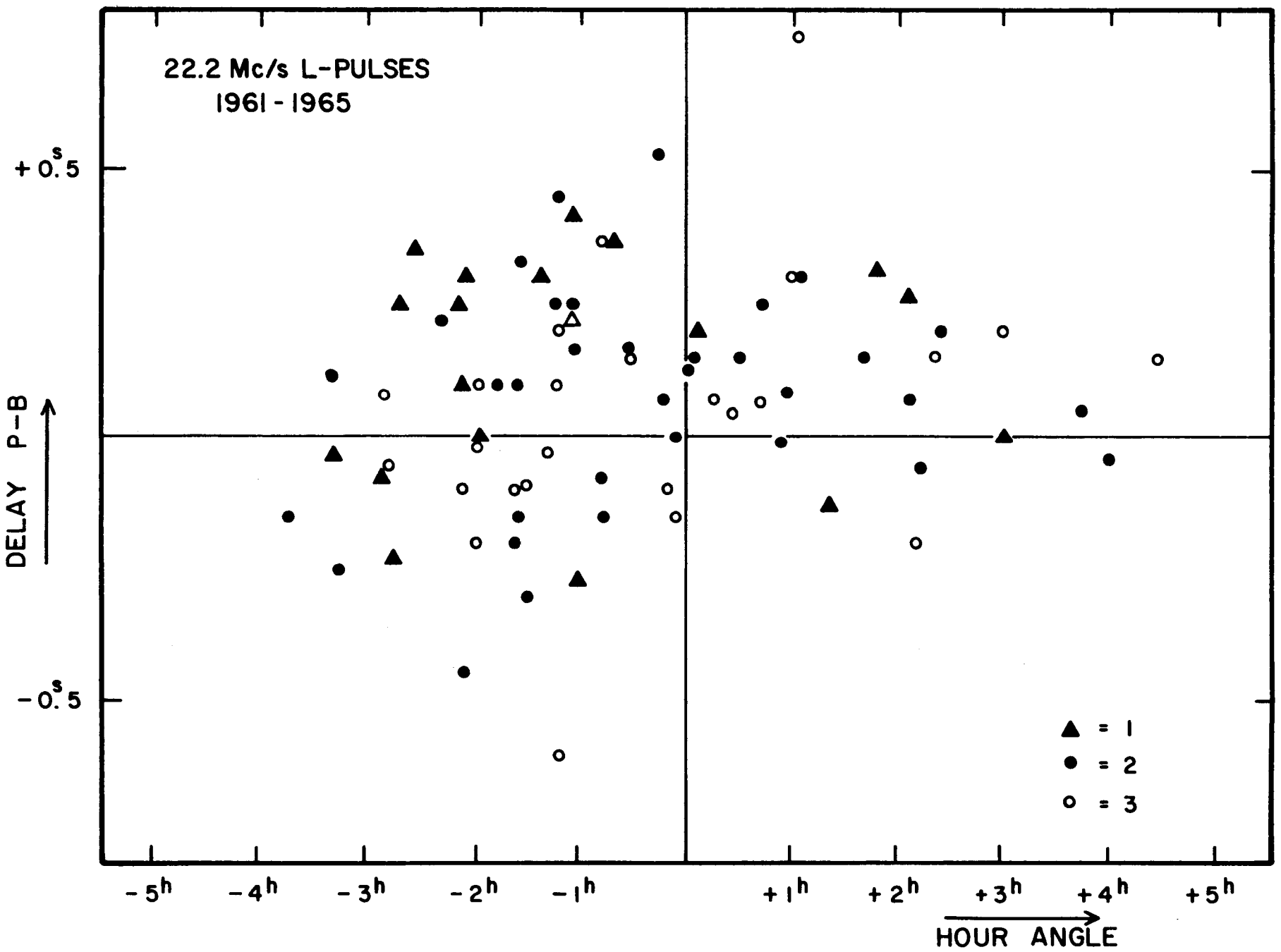
22.2 Mc/s L-PULSES
1961 - 1965
+0.s5
-0.s5
DELAY P-B
▲ = 1
● = 2
○ = 3
-5h
-4h
-3h
-2h
-1h
+1h
+2h
+3h
+4h
+5h
HOUR ANGLE